A New Method for Treating Drude Polarization in Classical Molecular Simulation

Alex Albaugh[1] and Teresa Head-Gordon[1,2,3,4*]

Departments of [1]Chemical & Biomolecular Engineering, [2]Chemistry, and [3]Bioengineering, [4]Chemical Sciences Division, Lawrence Berkeley National Laboratory, University of California, Berkeley, California 94720, United States

ABSTRACT

With polarization becoming an increasingly common feature in classical molecular simulation, it is important to develop methods that can efficiently and accurately evaluate the many-body polarization solution. In this work we expand the theoretical framework of our inertial extended Langrangian, self-consistent field iteration-free method (iEL/0-SCF), introduced for point induced dipoles, to the polarization model of a Drude oscillator. When applied to the polarizable simple point charge model (PSPC) for water, our iEL/0-SCF method for Drude polarization is as stable as a well-converged SCF solution and more stable than traditional extended Lagrangian (EL) approaches or EL formulations based on two temperature ensembles where Drude particles are kept "colder" than the real degrees of freedom. We show that the iEL/0-SCF method eliminates the need for mass repartitioning from parent atoms onto Drude particles, obeys system conservation of linear and angular momentum, and permits the extension of the integration time step of a basic molecular dynamics simulation to 6.0 fs for PSPC water.

*Corresponding author:
Stanley 274
510-666-2744 (V)
thg@berkeley.edu

INTRODUCTION

Force fields that include many-body polarization offer a model that, when adequately parameterized[1-2], is capable of greater accuracy and improved transferability, relative to their fixed charge counterparts[3]. This promise of better physics has led many research groups to take up polarization as a new advanced potential energy surface model[4], but implemented in very different functional forms including the Drude oscillator[5-11], the fluctuating charge model[12-17], and the induced dipole model[18-27]. While the polarization solution for the point induced dipole model is typically solved through self-consistent field (SCF) methods[28-30] or perturbation treatments[31-33], Drude and fluctuating charge models are typically solved through an extended Lagrangian (EL) formulation to eliminate the cost of the many SCF iterations needed to converge the polarization solution[8, 34-35].

Most recently we have developed a hybrid of an extended Lagrangian and an SCF solution to mutual polarization[36], which we have adapted from a time-reversible formulation of *ab initio* molecular dynamics introduced by Niklasson and colleagues[37-41]. Our "inertial EL/SCF" (iEL/SCF) approach is based on an extended set of auxiliary induced dipoles that are dynamically integrated so as to serve as a time-reversible initial guess for the SCF solution of the real induced dipoles. Subsequently we introduced a new iEL/SCF method that eliminates the need for any SCF calculations, which we call iEL/0-SCF (i.e. no self consistent field iterations), illustrated with the AMOEBA induced dipole model.[42] One of the main benefits of the iEL/0-SCF method is that the cost of evaluating mutual polarization is no more than the cost of the permanent electrostatics that is employed.

In this work we present the theory that extends the iEL/0-SCF approach to Drude polarization, in which we show that we eliminate the need for any mass repartitioning and thus temperature control in the two-temperature ensemble EL(T,T*) approaches used to solve Drude polarization[9], thereby yielding standard NVE and NVT ensembles, and illustrated with simulations using the polarizable simple point charge (PSPC) Drude model for bulk water[34]. We show that our iEL/0-SCF method for Drude polarization is as stable as a tightly converged SCF calculation and more stable than the EL(T,T*) approach. This greater stability allows us to take molecular dynamics timesteps as large as 6.0 fs while still preserving the properties of the PSPC model in the NVT ensemble.

THEORY

The PSPC model is a simple rigid water model[8-9], with partial charges on both hydrogens and oxygen, and a Lennard-Jones site and a Drude particle that is harmonically bound to each oxygen atom. The total energy of the PSPC model is then given by

$$U(\boldsymbol{r}^N) = U_{LJ}(\boldsymbol{r}^N) + \sum_i \sum_{j>i} \frac{q_i q_j}{|\boldsymbol{r_i} - \boldsymbol{r_j}|} + \sum_i \sum_j \frac{q_i q_{D,j}}{|\boldsymbol{r_i} - \boldsymbol{r_{D,j}}|} + \sum_i \sum_{j>i} \frac{q_{D,i} q_{D,j}}{|\boldsymbol{r_{D,i}} - \boldsymbol{r_{D,j}}|} + \frac{1}{2} k_D \sum_i |\boldsymbol{r_i} - \boldsymbol{r_{D,i}}|^2 \tag{1}$$

where $U_{LJ}(\boldsymbol{r}^N)$ is the standard Lennard-Jones term, the second through fourth terms are the electrostatic energy broken down into charge-charge, charge-Drude, and Drude-Drude interactions, respectively. The final term is the harmonic spring between Drude particles and their parent oxygen atom, where a Drude spring force constant, k_D, of 1000 kcal/mol/Å is employed in the PSPC model.

The relationship between the Drude spring force constant, k_D, polarizability, α, and Drude charge, q_D, can be easily derived and is given by

$$\alpha = \frac{q_D^2}{k_D} \tag{2}$$

The energy minima with respect to Drude displacements from their parent atom, $\boldsymbol{d_i} = \boldsymbol{r_{D,i}} - \boldsymbol{r_i}$, is

$$\frac{\partial U}{\partial \boldsymbol{r}_{D,i}} = k_D \boldsymbol{d_i} - q_{D,i} \boldsymbol{E}_{D,i}(\boldsymbol{d}^N) = 0 \tag{3}$$

where $\boldsymbol{E}_i(\boldsymbol{d}^N)$ is the electric field at site *i* due to the other atomic charges and Drude particles in the system. Eq. (3) states that the system's polarization energy is minimized when there is no net force on the Drude particles, and it defines the iterative equation that must be solved to determine the SCF solution for the Drude model.

Following generalized time reversible Born-Oppenheimer dynamics[37-38] and its application to classical dipolar polarization[42], we begin by defining a new extended Lagrangian for the Drude PSPC polarization model, given by Eq. (4).

$$\begin{aligned} \mathcal{L}(\boldsymbol{r}^N, \dot{\boldsymbol{r}}^N, \boldsymbol{a}_D^N, \dot{\boldsymbol{a}}_D^N) \\ &= \frac{1}{2} \sum_i m_i |\dot{\boldsymbol{r}}_i|^2 - U_{LJ}(\boldsymbol{r}^N) - \sum_i \sum_{j>i} \frac{q_i q_j}{|\boldsymbol{r_i} - \boldsymbol{r_j}|} - \sum_i \sum_j \frac{q_i q_{D,j}}{|\boldsymbol{r_i} - \boldsymbol{r_{D,j}}(\boldsymbol{a}_D^N)|} \\ &- \sum_i \sum_{j>i} \frac{q_{D,i} q_{D,j}}{|\boldsymbol{r_{D,i}}(\boldsymbol{a}_D^N) - \boldsymbol{r_{D,j}}(\boldsymbol{a}_D^N)|} - \frac{1}{2} k_D \sum_i |\boldsymbol{r_i} - \boldsymbol{a_{D,i}}(\boldsymbol{a}_D^N)|^2 \\ &- \tfrac{1}{2} m_a \textstyle\sum_i |\dot{\boldsymbol{a}}_{D,i}|^2 - \tfrac{1}{2} \omega^2 m_a \textstyle\sum_i |\boldsymbol{r}_{D,i}^{SCF} - \boldsymbol{a}_{D,i}|^2 \end{aligned} \tag{4}$$

The first six terms (kinetic energy, Lennard-Jones potential, Coulombic terms, and harmonic force between the Drude and parent atom) largely recapitulate Eq. (1), but with several important exceptions when formulated within our iEL/SCF hybrid approach: (1) we introduce an extended system of auxiliary Drude positions, $\boldsymbol{a}_{D,i}$, as dynamic degrees of freedom which have an associated fictitious mass, m_a; (2) this in turn gives rise to a positional dependence of the real Drude particles on these

auxiliary degrees of freedom, $\boldsymbol{r_{D,i}}(\boldsymbol{a}_D^N)$ and (3) a new kinetic energy term for the auxiliary degrees of freedom; and (4) a harmonic coupling between the auxiliary positions and the true SCF converged position, $\boldsymbol{r}_{\boldsymbol{D,i}}^{SCF}$. The strength of this coupling is controlled by the parameter ω, which should be as high as possible; it has been shown that the highest stable value of ω for a Verlet integration scheme is $\sqrt{2}/\Delta t$, where Δt is the time step.[37]

We now recognize that the most general form of the potential energy for the original Drude model from Eq. (4) is,

$$U(\boldsymbol{r}^N, \boldsymbol{a}_D^N) = U_{LJ}(\boldsymbol{r}^N) + \sum_i \sum_{j>i} \frac{q_i q_j}{|\boldsymbol{r_i} - \boldsymbol{r_j}|} + \sum_i \sum_j \frac{q_i q_{D,j}}{|\boldsymbol{r_i} - \boldsymbol{r_{D,j}}(\boldsymbol{a}_D^N)|} + \sum_i \sum_{j>i} \frac{q_{D,i} q_{D,j}}{|\boldsymbol{r_{D,i}}(\boldsymbol{a}_D^N) - \boldsymbol{r_{D,j}}(\boldsymbol{a}_D^N)|} + \frac{1}{2} k_D \sum_i |\boldsymbol{r_i} - \boldsymbol{r_{D,i}}(\boldsymbol{a}_D^N)|^2 \tag{5}$$

i.e. since the Drude positions depend explicitly on the auxiliary Drude positions, there is no assumption that the potential energy $U(\boldsymbol{r}^N, \boldsymbol{a}_D^N)$ is at the ground state solution as per Eq. (3). The positional dependence of the real Drude particles on the auxiliary degrees of freedom, $\boldsymbol{r_{D,i}}(\boldsymbol{a}_D^N)$, is formulated by making one evaluation of the electric field using the auxiliary positions as the positions of the Drude particles,

$$\boldsymbol{r_{D,i}}(\boldsymbol{a}_D^N) = \frac{q_{D,i}}{k_D} \boldsymbol{E}_{D,i}(\boldsymbol{a}_D^N) + \boldsymbol{r}_i \tag{6}$$

and which can be more specifically constituted for the PSPC model in Eq. (7).

$$\boldsymbol{r}_{D,i}(\boldsymbol{a}_D^N) = -\frac{q_{D,i}}{k_D} \left[\sum_j \frac{q_j(\boldsymbol{a}_{D,i} - \boldsymbol{r}_j)}{|\boldsymbol{a}_{D,i} - \boldsymbol{r}_j|^3} + \sum_j \frac{q_j(\boldsymbol{a}_{D,i} - \boldsymbol{a}_{D,j})}{|\boldsymbol{a}_{D,i} - \boldsymbol{a}_{D,j}|^3} \right] + \boldsymbol{r}_i \tag{7}$$

It is important to emphasize why the Drude oscillator model is different than an induced dipole model in an SCF process. For the induced dipole model, the electric field due to other permanent charges or multipoles in the system is defined at an atomic center. This direct component of the electric field will not change throughout an iterative procedure because the atomic positions do not change; it is only the field due to other induced dipoles in the system that will change throughout an iterative procedure. This is not true of a Drude model. In a Drude model, the electric field at the Drude particles due to both the permanent multipoles and other Drude particles will change because the position where we need to evaluate the electric field itself changes throughout the iterative process. We can see this explicitly in Eq. (7) where the first term in the bracket can be thought of as a direct electric field and

the second term as a mutual electric field, but for both terms they show that the optimized Drude positions depend specifically on the auxiliary Drude positions.

We can now use Eq. (5) to compact the description of the Lagrangian in Eq. (4).

$$\mathcal{L}(\boldsymbol{r}^N, \dot{\boldsymbol{r}}^N, \boldsymbol{a}_D^N, \dot{\boldsymbol{a}}_D^N) = \frac{1}{2}\sum_i m_i|\dot{\boldsymbol{r}}_i|^2 + \frac{1}{2}m_a\sum_i\left|\dot{\boldsymbol{a}}_{D,i}\right|^2 - \frac{1}{2}\omega^2 m_a\sum_i\left|\boldsymbol{r}_{D,i}^{SCF} - \boldsymbol{a}_{D,i}\right|^2 - U(\boldsymbol{r}^N, \boldsymbol{a}_D^N) \tag{8}$$

in order to apply the Euler-Lagrange equation of motion, in order to obtain equations of motion for both the real coordinates $\boldsymbol{r}^N$ and the auxiliary dipoles $\boldsymbol{a}_D^N$.

For our original iEL/SCF approach, the auxiliary positions would be used as an initial guess for a subsequent SCF calculation to the converged solution. The need for additional SCF iterations is undesirable especially for the Drude formulation since now the direct part of the electric field has to be evaluated at each iteration as described above and also because of the additional cost associated with iteration. However, in the iEL/0-SCF approach, we avoid the SCF by introducing a linear mixing of real and auxiliary Drude positions as an approximation to the ground state solution:

$$\boldsymbol{r}_{D,i}^{SCF} \approx \gamma\boldsymbol{r}_{D,i} + (1-\gamma)\boldsymbol{a}_{D,i} \tag{9}$$

Eq. (9) can be viewed as a predictor-corrector scheme[43] to serve as an approximation to the SCF solution, but is *only* used to derive the first equation of motion for the auxiliary degrees of freedom when taking the limit of $m_a \to 0$

$$\ddot{\boldsymbol{a}}_i = \gamma\omega^2(\boldsymbol{r}_{D,i} - \boldsymbol{a}_{D,i}) \tag{10}$$

Two points are worth mentioning at this juncture: (1) the predictor-corrector form of the converged solution in Eq. (9) is not used for the calculation of the polarization energy and forces, but only applies to the derivation of the auxiliary equation of motion in Eq. (10)[42]; (2) the Drude degrees of freedom now have no mass and thus there is no mass repartitioning in our approach.

The equation of motion for the auxiliaries is straightforward, simply taking the form of harmonic motion about the real Drude positions. This introduces one free parameter, γ, that controls the mixing of the real and auxiliary Drude positions, and can be easily determined as we show in the Methods section and supplementary information (SI) material. The equation of motion for the atomic centers looks like the usual real particle equation of motion,

$$m_i\ddot{\boldsymbol{r}}_i = -\frac{dU(\boldsymbol{r}^N, \boldsymbol{a}_D^N)}{d\boldsymbol{r}_i}\bigg|_{\boldsymbol{a}_D^N} \tag{11}$$

where we note again that, unlike the usual EL schemes, the atomic mass m_i has not been reduced through repartitioning. The total potential derivative with respect to position is shown in Eq. (12)

$$\frac{dU(\boldsymbol{r}^N,\boldsymbol{a}_D^N)}{d\boldsymbol{r}_i} = \frac{\partial U(\boldsymbol{r}^N,\boldsymbol{a}_D^N)}{\partial \boldsymbol{r}_i} + \sum_j \frac{\partial U(\boldsymbol{r}^N,\boldsymbol{a}_D^N)}{\partial \boldsymbol{r}_{D,j}} \frac{\partial \boldsymbol{r}_{D,j}}{\partial \boldsymbol{r}_i} \tag{12}$$

where the first term corresponds to the usual gradient terms for a standard EL scheme and the second term is a Drude 'response' term, which is normally not evaluated under an SCF approach since it goes to 0 in the limit of complete convergence. However, since the form of the potential, $U(\boldsymbol{r}^N,\boldsymbol{a}_D^N)$, is now general, i.e. it does not assume complete convergence, we must explicitly evaluate the response terms to ensure that the potential and potential gradient are commensurate. These response terms, described in more detail below, do have an additional cost, which is approximately the same as a single iterative step. But since we are doing no additional iterations, this is just a small cost overhead, especially when compared to a naïve successive over-relaxation (SOR)[28] method that requires ~20 iterations to achieve convergence.

The force vectors $\frac{\partial U(\boldsymbol{r}^N,\boldsymbol{a}_D^N)}{\partial \boldsymbol{r}_i}$ and $\frac{\partial U(\boldsymbol{r}^N,\boldsymbol{a}_D^N)}{\partial \boldsymbol{r}_{D,j}}$ are already evaluated in a standard Drude oscillator simulation, so we can easily calculate these force vectors. The first of these vectors, $\frac{\partial U(\boldsymbol{r}^N,\boldsymbol{a}_D^N)}{\partial \boldsymbol{r}_i}$, is simply the (negative) of the net force acting on the i^{th} atom. This force will be due to Lennard-Jones, Coulombic, and harmonic spring interactions. The second of these vectors, $\frac{\partial U(\boldsymbol{r}^N,\boldsymbol{a}_D^N)}{\partial \boldsymbol{r}_{D,j}}$, is just the (negative) of the net force acting on the j^{th} Drude particle, which will just be comprised of standard Coulombic and harmonic spring interactions. The new additional term, $\frac{\partial \boldsymbol{r}_{D,j}}{\partial \boldsymbol{r}_i}$, when expanded, is

$$\frac{\partial \boldsymbol{r}_{D,i}}{\partial \boldsymbol{r}_k} = -\frac{q_{D,i}}{k_D}\left[\sum_j \frac{\partial}{\partial \boldsymbol{r}_k}\left(\frac{q_j(\boldsymbol{a}_{D,i}-\boldsymbol{r}_j)}{|\boldsymbol{a}_{D,i}-\boldsymbol{r}_j|^3}\right) + \sum_j \frac{\partial}{\partial \boldsymbol{r}_k}\left(\frac{q_j(\boldsymbol{a}_{D,i}-\boldsymbol{a}_{D,j})}{|\boldsymbol{a}_{D,i}-\boldsymbol{a}_{D,j}|^3}\right)\right] + \frac{\partial \boldsymbol{r}_i}{\partial \boldsymbol{r}_k}$$

$$= \frac{q_{D,i}}{k_D}\sum_j q_j \frac{\partial}{\partial \boldsymbol{r}_k}\left(-\frac{(\boldsymbol{a}_{D,i}-\boldsymbol{r}_j)}{|\boldsymbol{a}_{D,i}-\boldsymbol{r}_j|^3}\right) + \delta_{ik}\boldsymbol{I} \tag{13}$$

One can recognize that the derivative term within the sum of Eq. (13) is actually the definition of a dipole interaction tensor, $\boldsymbol{T}$, between the k atomic center, $\boldsymbol{r}_k$, and the i^{th} auxiliary Drude position, $\boldsymbol{a}_{D,i}$, to yield Eq. (14).

$$\frac{\partial \boldsymbol{r}_{D,i}}{\partial \boldsymbol{r}_k} = \frac{q_{D,i}}{k_D}\boldsymbol{T}_{a_D i,k} q_k + \delta_{ik}\boldsymbol{I} \tag{14a}$$

where

$$\boldsymbol{T}_{a_D i,k} = \begin{bmatrix} \frac{3\left(a_{D,i}^{x}-r_k^{x}\right)^2}{\left|\boldsymbol{a}_{D,i}-\boldsymbol{r}_k\right|^5} - \frac{1}{\left|\boldsymbol{a}_{D,i}-\boldsymbol{r}_k\right|^3} & \frac{3\left(a_{D,i}^{x}-r_k^{x}\right)\left(a_{D,i}^{y}-r_k^{y}\right)}{\left|\boldsymbol{a}_{D,i}-\boldsymbol{r}_k\right|^5} & \frac{3\left(a_{D,i}^{x}-r_k^{x}\right)\left(a_{D,i}^{z}-r_k^{z}\right)}{\left|\boldsymbol{a}_{D,i}-\boldsymbol{r}_k\right|^5} \\ \frac{3\left(a_{D,i}^{x}-r_k^{x}\right)\left(a_{D,i}^{y}-r_k^{y}\right)}{\left|\boldsymbol{a}_{D,i}-\boldsymbol{r}_k\right|^5} & \frac{3\left(a_{D,i}^{y}-r_k^{y}\right)^2}{\left|\boldsymbol{a}_{D,i}-\boldsymbol{r}_k\right|^5} - \frac{1}{\left|\boldsymbol{a}_{D,i}-\boldsymbol{r}_k\right|^3} & \frac{3\left(a_{D,i}^{y}-r_k^{y}\right)\left(a_{D,i}^{z}-r_k^{z}\right)}{\left|\boldsymbol{a}_{D,i}-\boldsymbol{r}_k\right|^5} \\ \frac{3\left(a_{D,i}^{x}-r_k^{x}\right)\left(a_{D,i}^{z}-r_k^{z}\right)}{\left|\boldsymbol{a}_{D,i}-\boldsymbol{r}_k\right|^5} & \frac{3\left(a_{D,i}^{y}-r_k^{y}\right)\left(a_{D,i}^{z}-r_k^{z}\right)}{\left|\boldsymbol{a}_{D,i}-\boldsymbol{r}_k\right|^5} & \frac{3\left(a_{D,i}^{z}-r_k^{z}\right)^2}{\left|\boldsymbol{a}_{D,i}-\boldsymbol{r}_k\right|^5} - \frac{1}{\left|\boldsymbol{a}_{D,i}-\boldsymbol{r}_k\right|^3} \end{bmatrix} \tag{14b}$$

Substituting Eq. (14) into Eq. (12) we obtain Eq. (15),

$$\frac{dU\left(\boldsymbol{r}^{\boldsymbol{N}},\boldsymbol{a}_{\boldsymbol{D}}^{\boldsymbol{N}}\right)}{d\boldsymbol{r}_i} = \frac{\partial U\left(\boldsymbol{r}^{\boldsymbol{N}},\boldsymbol{a}_{\boldsymbol{D}}^{\boldsymbol{N}}\right)}{\partial \boldsymbol{r}_i} + \sum_j \frac{\partial U\left(\boldsymbol{r}^{\boldsymbol{N}},\boldsymbol{a}_{\boldsymbol{D}}^{\boldsymbol{N}}\right)}{\partial \boldsymbol{r}_{D,j}}\left(\frac{q_{D,j}q_i}{k_D}\boldsymbol{T}_{a_D j,i} + \delta_{ji}\boldsymbol{I}\right) \tag{15}$$

the working definition of the atomic center gradients that are used to drive the molecular dynamics updates of positions and velocities for the atomic and Drude particles. It should be noted that the introduction of the dipole interaction tensor, $\boldsymbol{T}$, that follows from our theory are not always available from community codes that are currently restricted to point charges and point charge-only Ewald calculations. For this work we modified the Tinker8 software package[44] to use Drude polarization instead of its usual induced point dipole formalism; Tinker8 already has code to handle the dipole interaction tensor and higher-order multipolar Ewald sums, meaning that much of the software infrastructure to properly evaluate Eq. (15) is already in place.

METHODS

Three different methods for solving the Drude polarization condition in Eq. (3) were then implemented for comparison purposes- an SCF solver, the iEL/0-SCF method described above, and the EL(T,T*) method based on the two temperature NPT,T* ensemble described by Lamoureux and Roux for the PSPC model[9]. The SCF solver is a naïve successive over-relaxation (SOR) method[28] that iterates Eq. (3) to within some defined tolerance in terms of the root mean square change in force on the Drude particles between successive iterations. A range of tolerances were tested with the tightest being 10^{-6} RMS kcal/mol/Å, which we define as the 'gold standard' for accuracy in this study.

The EL(T,T*) method for polarization was originated by Sprik[45], and was used by Wodak and colleagues for point induced dipoles[34] and by Lamoureux and Roux for Drude polarization[9]. Under the EL(T,T*) scheme the Drude particles themselves are given a portion of the mass of their parent atom, m_D, and to conserve mass the parent atom now has a mass of $m_i - m_D$. The Lagrangian of the system then becomes

$$\mathcal{L}(\boldsymbol{r}^N, \dot{\boldsymbol{r}}^N, \boldsymbol{r}_D^N, \dot{\boldsymbol{r}}_D^N) = \frac{1}{2}\sum_i (m_i - m_D)|\dot{\boldsymbol{r}}_i|^2 + \frac{1}{2}m_D \sum_i \left|\dot{\boldsymbol{r}}_{D,i}\right|^2 - U_{LJ}(\boldsymbol{r}^N) - \sum_i \sum_{j>i} \frac{q_i q_j}{|\boldsymbol{r}_i - \boldsymbol{r}_j|} - \sum_i \sum_j \frac{q_i q_{D,j}}{|\boldsymbol{r}_i - \boldsymbol{r}_{D,j}|}$$
$$- \sum_i \sum_{j>i} \frac{q_{D,i} q_{D,j}}{|\boldsymbol{r}_{D,i} - \boldsymbol{r}_{D,j}|} - -\frac{1}{2}k_D \sum_i \left|\boldsymbol{r}_i - \boldsymbol{r}_{D,i}\right|^2 \tag{16}$$

Where the last five terms give the potential energy of the system and the Lagrangian can be simplified as

$$\mathcal{L}(\boldsymbol{r}^N, \dot{\boldsymbol{r}}^N, \boldsymbol{r}_D^N, \dot{\boldsymbol{r}}_D^N) = \frac{1}{2}\sum_i (m_i - m_D)|\dot{\boldsymbol{r}}_i|^2 + \frac{1}{2}m_D \sum_i \left|\dot{\boldsymbol{r}}_{D,i}\right|^2 - U(\boldsymbol{r}^N, \boldsymbol{r}_D^N) \tag{17}$$

Applying the Euler-Lagrange equation of motion we now obtain equations of motion for atomic centers and Drude particles in Eqs. (18a) and (18b), respectively.

$$(m_i - m_D)\ddot{\boldsymbol{r}}_i = -\frac{dU}{d\boldsymbol{r}_i} \tag{18a}$$

$$m_D \ddot{\boldsymbol{r}}_{D,i} = -\frac{dU}{d\boldsymbol{r}_{D,i}} \tag{18b}$$

In short, the dynamics of the atomic centers are driven by their usual forces, but with a smaller mass, and a net force now drives the dynamics of the Drude particles given by the harmonic spring attaching it to its parent atom and an electrostatic force through interactions with its charge and the charges of the rest of the system.

In the NVT,T* or NPT,T* ensemble of the EL(T,T*) method[45], the atomic temperature T is defined by the total atomic mass m_i and the center of mass velocity of the Drude-parent atom pair *i*, $\dot{\boldsymbol{R}}_i$.

$$T = \frac{1}{3k_B N_{atom}} \sum_{i \in atom} \frac{\left|m_i \dot{\boldsymbol{r}}_i + m_D \dot{\boldsymbol{r}}_{D,i}\right|^2}{m_i} = \frac{1}{3k_B N_{atom}} \sum_{i \in atom} m_i \dot{\boldsymbol{R}}_i^2 \tag{19}$$

where N_{atomic} is the number of atomic centers. The Drude particles are kept at a lower temperature T*, defined by the reduced mass and the relative velocity of the Drude-parent atom pair, m_i' and $\dot{\boldsymbol{d}}_i$, respectively.

$$T^* = \frac{1}{3k_B N_{Drude}} \sum_{i \in Drude} m_D \left(1 - \frac{m_D}{m_i}\right) \left|\dot{\boldsymbol{r}}_{D,i} - \dot{\boldsymbol{r}}_i\right|^2 = \frac{1}{3k_B N_{Drude}} \sum_{i \in Drude} m_i' \dot{\boldsymbol{d}}_i^2 \tag{20}$$

where N_{Drude} is the number of Drude centers. By keeping the Drude temperature low, kinetic energy is bled out to better satisfy the Born-Oppenheimer condition.

For the iEL/0-SCF and EL(T,T*) methods the Drude positions and auxiliaries were initialized to those of a tight SCF solution, and all production simulations were started from pre-equilibrated restart files; unless noted otherwise all simulations (NVT or NVE) are initialized at 298.0 K. For all methods all equations of motion were integrated with a velocity Verlet scheme[46] and we used particle-mesh Ewald summation to treat all electrostatic interactions[47] with a real-space cutoff of 9.0 Å. Non-bonded interactions were evaluated using neighbor lists and intra-molecular geometry of the PSPC model was constrained using the RATTLE algorithm[48]. When thermostats are used, either to perform NVT simulations or to couple to auxiliaries (for iEL/0-SCF) or relative Drude-parent atom harmonic motion (for EL(T,T*)), a time-reversible 4th-order Nosé-Hoover chain[49] was used with a thermostat time scale parameter of 0.005 ps (expect for the EL method at a time step of 4.0 fs, which uses a time scale parameter of 0.01 ps, as 0.005 ps is unstable at that condition) . All three methods were tested over a range of time steps, ranging from 0.5 fs to 6.0 fs depending on method.

The iEL/0-SCF method requires the determination of an optimal value of γ, the mixing parameter that allows us to approximate a ground state polarization solution that will deviate from the true solution by a quantity, δ. We have shown in previous work that the iEL/0-SCF is numerically stable over long simulation times because the general form of the polarization energy and forces (Eqs. (5) and (12) for the Drude model) ensures that small deviations from the converged solution only gives rise to errors on the order of $O(\delta^2)$ in energy and forces.[42] Thus the mixing parameter γ will control the level of accuracy of the polarization solution and corresponding stability of the equations of motion.

In our previous work with the AMOEBA force field[36, 42], we determined γ by looking for a value that best conserved the real system energy while minimizing the auxiliary "temperature" drift rate that arises from resonances (we refer the reader to the original formulation of the iEL/SCF method[36] for further detail). For AMOEBA, we found an optimal $\gamma = 0.9$ value for water using a 0.5 fs time step in the NVE ensemble, with values of the time step greater than 0.5 fs and $\gamma > 0.9$ displaying unstable trajectories, and values of $\gamma < 0.5$ yielding very poor real system energy conservation regardless of time step.[42] As shown in Figure S1-S3, the Drude model allows for a far greater range of γ values and a time step of up to 2.0 fs for which the NVE trajectory is both stable and exhibits good energy conservation comparable to or better than the SCF solution. We adopted a value of $\gamma = 1$ for all simulations reported in the Results section, indicating that the Drude positions calculated directly from the auxiliaries are of a high enough quality so as to drive the auxiliary equation of motion close to the true ground state with no additional correction as per Eq. (9).

RESULTS

For the iEL/SCF methods, the equations of motion of the Drude particles given in Eq. (10) are defined in the limit $m_a \rightarrow 0$, so there are no contributions to the real system energy due to the kinetic energy of the Drude particles. This is equivalent to an SCF scheme under tight convergence (which we take to be 10^{-6} RMS kcal/mol/Å), but is unlike an EL method where there is mass repartitioning between the Drude particle and its parent atom. For EL, the assignment of small Drude masses are preferred for energy conservation by minimizing the Drude kinetic energy (the Born-Oppenheimer condition) but the simulation is restricted to short time steps due to their higher frequency oscillations (since $\omega = \sqrt{k_D/m_D}$). By contrast larger masses in the EL scheme that allow for longer time steps tend to conserve energy more poorly due to the increasing Drude kinetic energy contribution. In what follows we report results in the EL method using the lowest stable Drude mass, m_D, for a given time step.

In the NVE ensemble, since we are not enforcing temperature control through thermostats, the two extended Lagrangian approaches simplify to just the equivalent of EL/0-SCF (no inertial restraints) and EL methods. Figure S4 shows that the system energy, i.e. the sum of all kinetic and potential energy of atomic and Drude particle contributions, for both EL approaches is as well conserved as the SCF gold standard at a time step of 1.0 fs over a 2.0 ns timescale. Figure 1a shows that while the EL/0-SCF method also conserves energy using a 2.0 fs time step – in fact better than the SCF method over the 2.0 ns trajectory – the EL method conserves energy poorly after ~250 ps at the lowest Drude mass where stable trajectories are possible. If we restrict ourselves to the first couple of hundreds of picoseconds for the EL method, we can collect values of the diffusion constant at 298K that are in good agreement between the methods, 4.00 x10^{-5} cm^2/s (± 0.08, SCF), 4.06 x10^{-5} cm^2/s (± 0.08, EL/0-SCF), and 3.99 x10^{-5} cm^2/s (± 0.23, EL), and all of which are in agreement with previous reported results for the PSPC model[9].

The energy instability of EL after ~250 ps arises from the fact that even for small values of m_D the Drude particles will eventually reach thermal equilibrium with the rest of the system, and the kinetic energy of the Drude particles – which is formally zero for the SCF and EL/0-SCF methods – will increase over time for the EL method. To show this, Figure 1b reports the Drude temperature for the relative Drude-parent atom motion for the SCF and EL methods and the 'pseudo-temperature' of the auxiliary dipoles, defined as $T_{aux} = 1/3\langle \dot{\boldsymbol{a}}_i^2 \rangle$, for the EL/0-SCF method at the same 2.0 fs time step and simulated over 2.0 ns. The EL method shows exponential degradation, rising from near 0 K at the beginning of a simulation to almost the atomic temperature after 2 ns; this will be the case for the EL method even for smaller time steps where the same kinetic energy change will be evident but on a

longer simulation time scale. By contrast the EL/0-SCF and SCF methods show linear increases in inertia throughout the simulation due to accumulation of integration error. Of course the point of the EL(T,T*) approach is to arrest this energy redistribution by keeping the Drude thermostat cold to stay on the Born-Oppenheimer surface. But the NVE results are instructive as they are a harbinger for the fact the EL/0-SCF is intrinsically more stable than the EL method at a given time step and length of simulation, and comparable in quality to a well converged SCF solution.

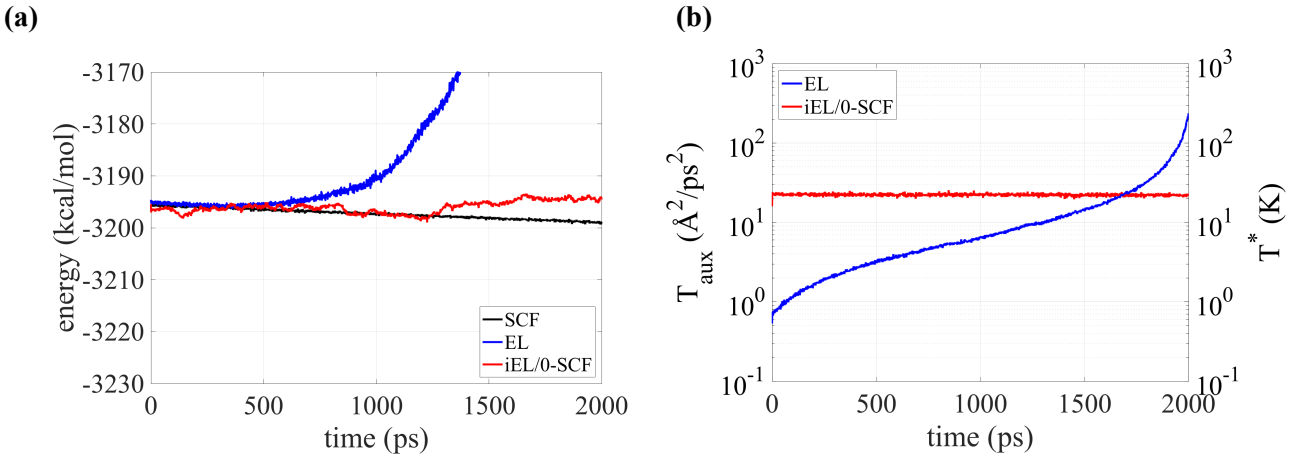

Figure 1*: NVE energy properties of the iEL/0SCF and EL(T,T*=0) method for the Drude PSPC model compared to the SCF reference.* All simulations were performed with a time step of 2.0 fs on a test system of 512 water molecules with no thermostats. (a) Total real system energy for SCF (black), iEL/0-SCF (red), and EL (blue) (b) auxiliary variables pseudo temperature for iEL/0-SCF (red, left axis) and temperature of the Drude-parent atom motion of the EL method (blue, right axis). Temperature is placed on a log scale.

We show that this continues to hold in the NVT ensemble by next considering the polarization properties of the PSPC model, where the atomic degrees of freedom are coupled to a Nosé-Hoover thermostat to maintain a temperature of 298K. Figure 2a shows the extended system conserved energy quantity, which differs for the three methods, using a 2.0 fs timestep. The conserved quantity for the SCF gold standard corresponds to all potential and kinetic energy terms of the atomic degrees of freedom and the atomic thermostats[49]. For the EL(T,T*) method the ensemble is NV(T,T*), since a cold T* thermostat of 1.0K is coupled to the Drude-parent atom relative motion, and thus its conserved energy quantity now includes both sets of thermostats. The iEL/0-SCF method also couples the pseudo temperature of the auxiliaries to a thermostat, but it is set to a pseudo temperature that conserves the extended system energy that includes the potential energy and kinetic energies of all the particles in the system, all of the auxiliary variable contributions, and the potential and kinetic energy of all the thermostats (atomic and auxiliary). I.e. the extended system energy conservation is enforced by construction with errors only associated with uncertainty in the linear fit.

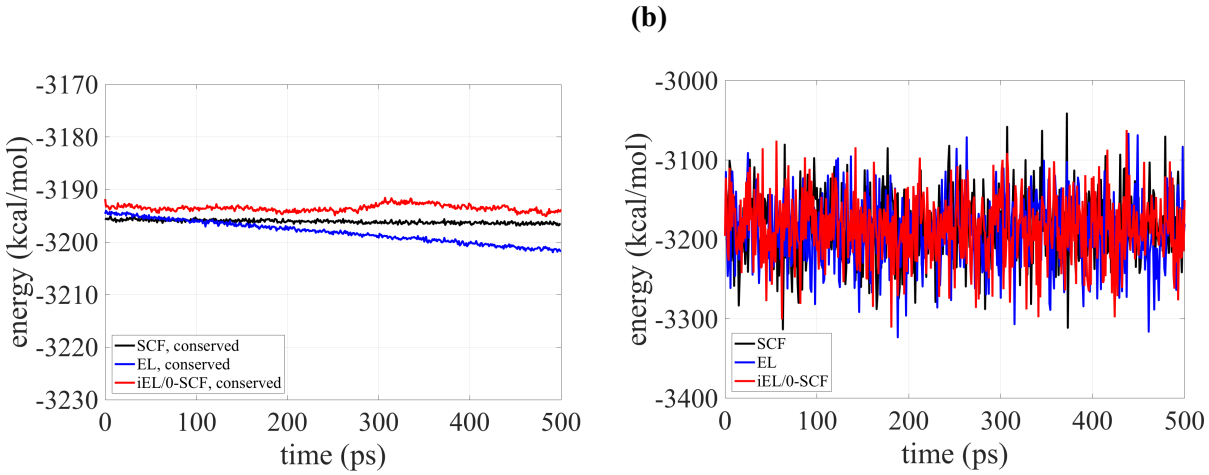

Figure 2: *NVT energy properties of the EL, SCF and iEL/0-SCF method for the Drude PSPC water model.* All simulations were performed with a time step of 2.0 fs on a test system of 512 water molecules. (a) The conserved quantity for the NVT extended system for the three methods, (b) the real system energy in the NVT ensemble at 298.0 K for SCF (black), EL(T*,T) (blue), and iEL/0-SCF (red). The system energy is the sum of the atomic kinetic and potential energies.

Table 1 shows that the the EL(T,T*) method has more drift in the conserved energy than does the SCF solution, although the real system energy and molecular dipole properties among the three methods are well reproduced at a 2.0 fs time step. However, the greater drift in the conserved energy quantity for EL(T,T*) indicates that it is becoming more sensitive to integration errors and thus limitations on allowed time steps compared to the SCF and iEL/0-SCF approaches.

Table 1. *Conserved extended energy drift, average system potential energy, and average molecular dipole of the PSPC model in the NVT ensemble for the SCF, EL and iEL/0-SCF methods at different integration time steps (fs).* $\langle U \rangle$ is the average system potential energy in kcal/mol, $\langle \mu_{mol} \rangle$ is the average molecular dipole in units of Debye, and $|\Delta E|/\Delta t$ is the extended system conserved energy quantity in kcal/mol/ps. For iEL/0-SCF the conserved quantity is enforced by construction. Results are from 1.0 ns simulations of 512 water molecules at 298K.

	SCF			**EL(T,T*)**			**iEL/0-SCF**	
Δt	$\langle \mu_{mol} \rangle$	$\langle U \rangle$	$\lvert \Delta E \rvert / \Delta t$	$\langle \mu_{mol} \rangle$	$\langle U \rangle$	$\lvert \Delta E \rvert / \Delta t$	$\langle \mu_{mol} \rangle$	$\langle U \rangle$
1.0	2.71 ± 0.01	-4110 ± 35	-0.0011	2.71 ± 0.01	-4110 ± 35	-0.0023	2.71 ± 0.01	-4110 ± 35
2.0	2.71 ± 0.01	-4100 ± 35	-0.0017	2.71 ± 0.01	-4100 ± 35	-0.014	2.71 ± 0.01	-4100 ± 35
3.0	2.71 ± 0.01	-4090 ± 35	-0.0037	2.71 ± 0.01	-4080 ± 35	-1.8	2.71 ± 0.01	-4080 ± 35
4.0	2.71 ± 0.01	-4070 ± 35	-0.0014	2.70 ± 0.01	-4070 ± 35	-81	2.70 ± 0.01	-4050 ± 35
5.0	2.70 ± 0.01	-4040 ± 35	-0.0027	---	---	---	2.70 ± 0.01	-4020 ± 35
6.0	2.69 ± 0.01	-4010 ± 35	+0.057	---	---	---	2.69 ± 0.01	-3990 ± 30
7.0	2.69 ± 0.01	-3970 ± 35	+1.0	---	---	---	2.69 ± 0.01	-3950 ± 35

This is confirmed in Figure 3a which plots the minimum Drude mass required to maintain a stable simulation as a function of increasing time step from 1.0 fs to 4.0 fs for the EL(T,T*) method

where T=298K and using a Drude-parent atom relative motion temperature T*= 1.0 K; beyond 4.0 fs the EL(T,T*) approach becomes unstable under any amount of mass repartitioning. As the integration time step increases, the repartitioned Drude mass must also increase, thereby becoming more and more untenable for accurately preserving the Born-Oppenheimer condition, which would manifest as evident degradation in polarization properties. This is seen in Figure 3b and 3c (as well as Figures S11 and S12) which reports the induced dipole distributions and induced dipole autocorrelation function at the 4.0 fs time step, in which ~25% of the mass of the parent oxygen atom is partitioned to the Drude oscillator, that are in significant disagreement with the SCF result.

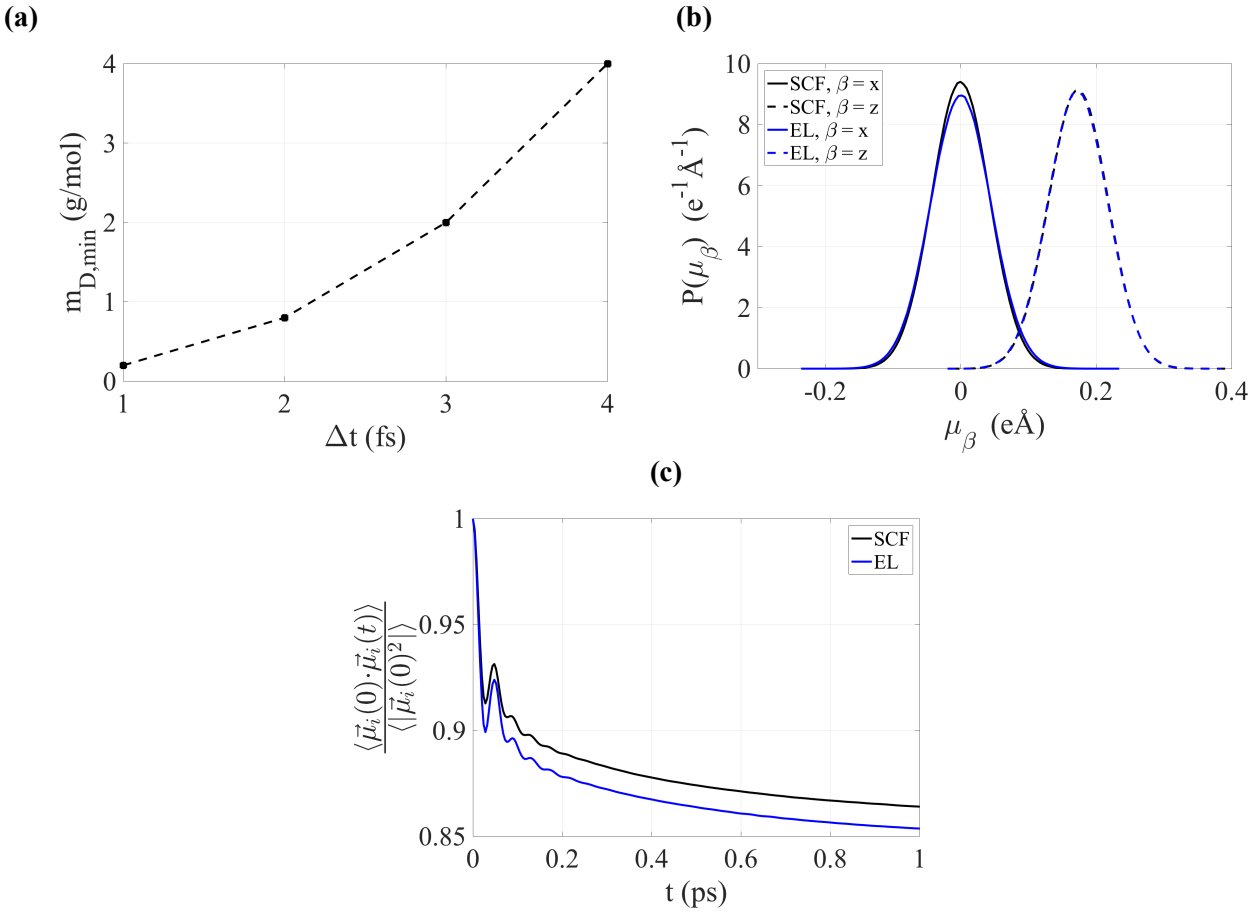

Figure 3: *Molecular dynamics trajectory stability and polarization properties of the PSPC model using the EL(T,T*) method.* (a) the minimum Drude mass required to maintain a stable MD simulation as a function of time step using a Drude-parent atom relative motion temperature set point of T*=1.0 K; the EL(T,T*) method is unstable above 4.0 fs. (b) probability density distributions and (c) autocorrelation function for the oxygen induced dipole, $\boldsymbol{\mu}_i = q_{D,i}(\mathbf{r}_{D,i} - \mathbf{r}_i)$ from the EL(T,T*) method compared to SCF at a 4.0 fs time step. All simulations were performed in the NVT ensemble at 298.0 K. All calculations presented in this figure use an internal coordinate system where the z-direction is given by the H-O-H bisector, the y-direction is out of the H-O-H plane, and the x-direction is orthogonal to z and y (see [50] for details).

By contrast, Figure 4a shows that the effective, fitted mass of the auxiliary Drude centers for the iEL/0-SCF method is ~2 orders of magnitude smaller than the repartitioned masses of the EL(T,T*) method, such that the effective temperature of the auxiliary degrees of freedom remain cold (<10K) for up to a 6.0 fs time step. Figure 4b and 4c show that the iEL/0-SCF method tracks the SCF result accurately for the induced dipole distributions and induced dipole autocorrelation function at the 4.0 fs time step, unlike the EL(T,T*) method. In fact, polarization properties are as well reproduced as the SCF solution all the way up to the 6.0 fs time step (Figure S10 and S11) and other properties generated by iEL/0-SCF, such as the radial distribution functions of the liquid, match the SCF result at this largest time step (Figure 5).

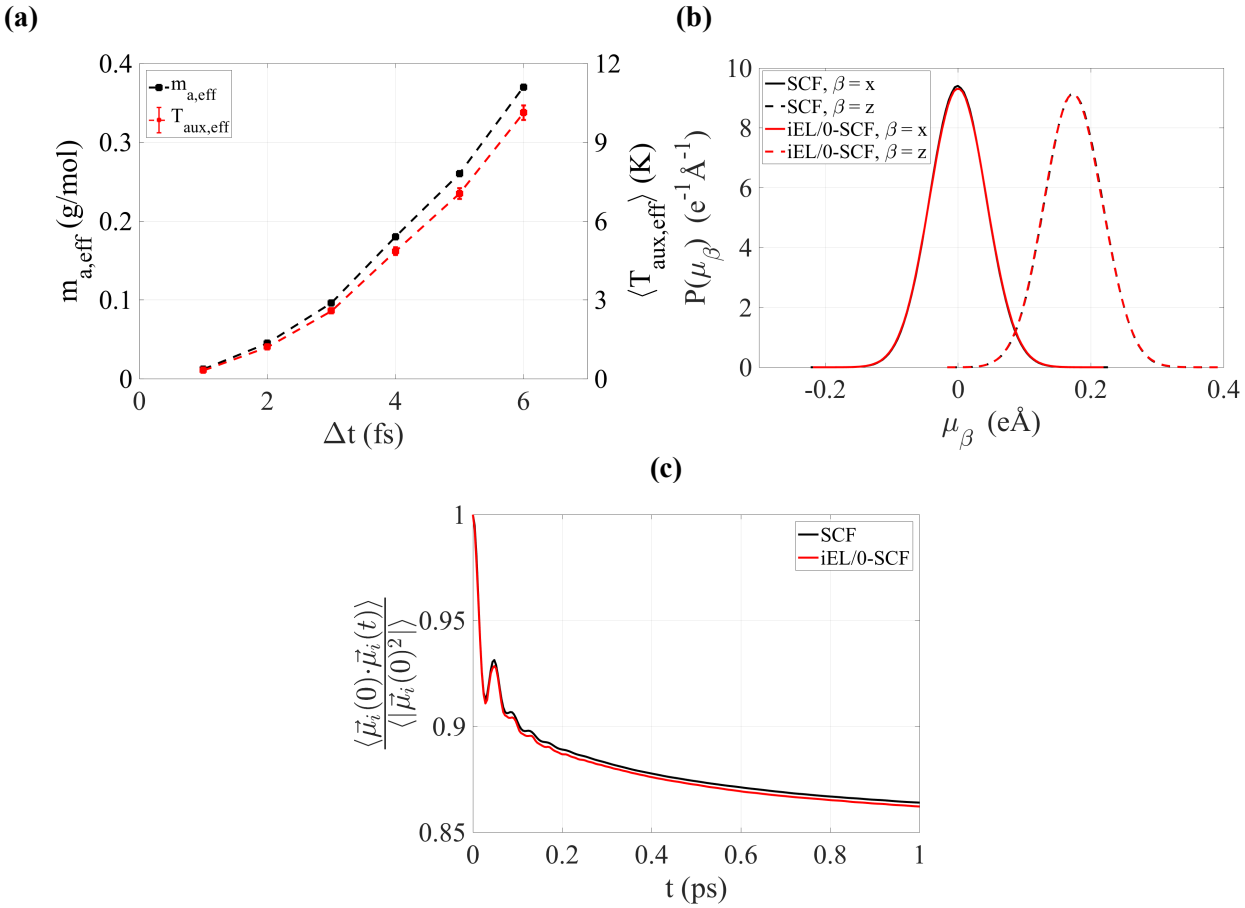

Figure 4: *Molecular dynamics trajectory stability and polarization properties of the PSPC model using the iEL/0-SCF method*. (a) The effective auxiliary mass, $m_{a,eff}$ (left axis) and the resultant auxiliary mean temperatures (right axis) using the effective masses to convert from pseudo temperature to real temperature for the iEL/0-SCF method. (b) probability density distributions and (c) autocorrelation function for the oxygen induced dipole, $\boldsymbol{\mu}_i = q_{D,i}(\mathbf{r}_{D,i} - \mathbf{r}_i)$ from the iEL/0-SCF method compared to SCF at a 4.0 fs time step. See Figure 3 for remaining details.

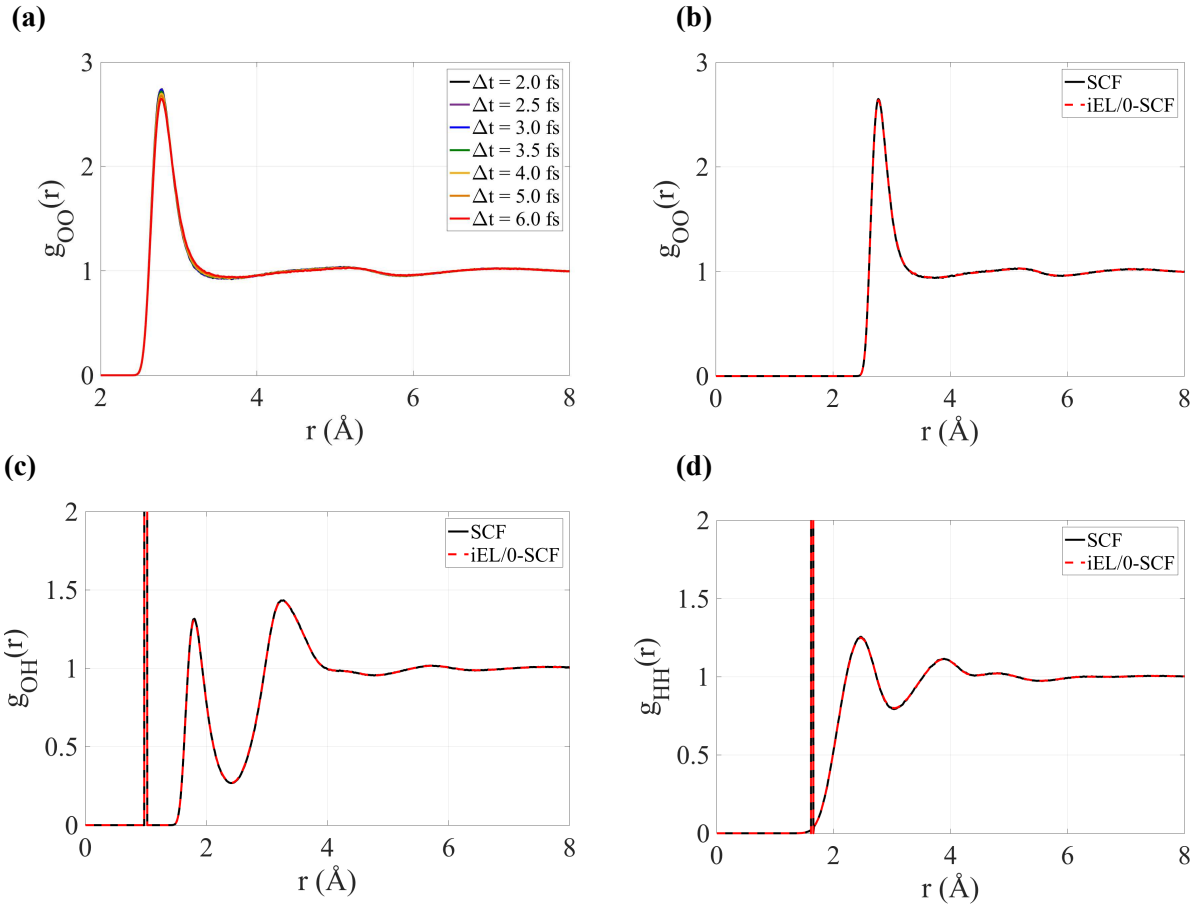

Figure 5: *Radial distribution functions (RDF) of the PSPC Drude water model using the SCF and iEL/0-SCF methods*. (a) oxygen-oxygen RDF as a function of time step for the SCF method showing small changes in the first peak as time step increases. Oxygen-oxygen RDF (b), oxygen-hydrogen RDF (c), and hydrogen-hydrogen RDF for the SCF method and iEL/0-SCF method. Simulations were run in the NVT ensemble at 298.0 K and were at least 0.5 ns in length. Panels (b), (c), and (d) used a time step of 6.0 fs.

Finally we consider why the iEL/0-SCF method is as good as an SCF solution although it requires no explicit SCF calculations at each time step. Our explanation is that the induced dipole updates, or equivalently the position updates of the real Drude particles by making one evaluation of the electric field using the current auxiliary positions, is performing a tightly converged SCF calculation on the fly. To bolster this argument, Figure 6a shows the autocorrelation function for the real dipoles and the single exponential fit to the initial decay, while Figure 6b reports the fitted time constant, as a function of the integration time step. Since the decay constant is on the order of a couple of hundred femtoseconds, the numerical integration of the auxiliary dipoles can "keep up" for adjusting the real dipole positions for time steps up to 6.0 fs to follow that longer time scale decay. We found that a 7.0 fs time step remained stable but properties of the PSPC model were beginning to degrade, and at 8.0 fs the simulation ultimately developed numerical instabilities after ~1 ns.

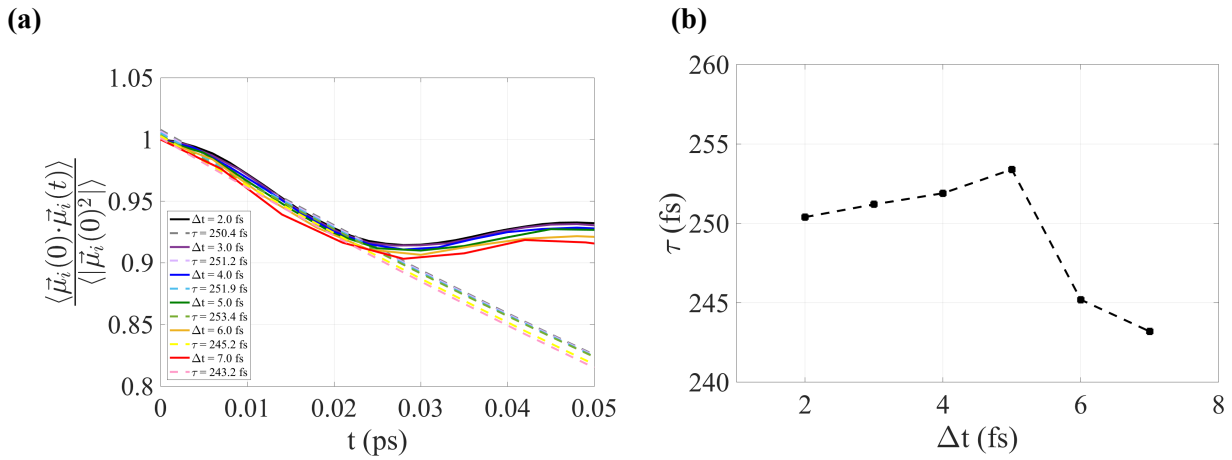

Figure 6: *The initial time scales for decay of the oxygen time autocorrelation for the real induced dipoles for the iEL/0-SCF method*. (a) single exponential fits (dotted lines) to the initial decay of the dipole created between the Drude and its parent atom, $\boldsymbol{\mu}_{D,i} = q_{D,i}(\mathbf{r}_{D,i} - \mathbf{r}_i)$ (solid lines), for a range of time steps. (b) the time constant of the exponential fit to the initial decay from (a) as a function of time step.

DISCUSSION AND CONCLUSION

We have developed a Drude implementation of our iEL/0-SCF method, which proves to be as accurate and stable for both dynamic and thermodynamic properties for the PSPC water model when compared to a tightly converged SCF solution, and a significant improvement over the two temperature EL(T,T*) approaches by increasing the allowable integration time step by a factor of 2-3 with recommended time steps as large as 6.0 fs. For iEL/0-SCF the better stability likely comes from the exact analytical agreement between the energy and gradients compared to SCF, and the avoidance of any mass repartitioning when compared to EL so that the Born-Oppenheimer condition is easily satisfied without needing to introduce two temperature ensembles. We therefore conclude that we gain the benefits of the minimal computational expense of an extended Lagrangian approach but with greatly increased time steps with the accuracy and robustness of an SCF method for Drude polarization. As we have noted in the Theory section, the addition of the iEL/0-SCF method to community codes would need to handle the dipole interaction tensor (Eq. (15)) and higher-order multipolar Ewald sums[47, 51]. Given that Amber and CHARMM have implemented the AMOEBA model, the software to implement the iEL/0-SCF approach is largely in place in these community codes.

It is interesting to analyze why the AMOEBA polarizable model for water is restricted to a time step that is a factor of 6 times smaller than the PSPC model using the iEL/0-SCF approach which we attribute to the following: (1) the PSPC has a rigid and not a flexible geometry like AMOEBA, (2) it does not include a Drude particle on the light hydrogen centers, unlike the AMOEBA model which

includes point dipoles on hydrogens, (3) PSPC has no intramolecular polarization, and (4) nor does PSPC have short ranged and a spatially rapid variation in forces arising from dipole and quadrupole permanent electrostatics. Thus the simplicity of the PSPC water model is better able to conform its motion on the Born-Oppenheimer surface using much longer time steps based on a simpler design choice of the polarizable and electrostatic model.

It therefore would also be expected that for a polarizable Drude model for a protein with flexible bonds or a 4-site Drude polarizable water model that places Drude particles on light hydrogens that the time step of 6 fs achieved with the PSPC model would need to decrease. However, there is a possibility that a time reversible integration of an auxiliary system could nonetheless help bootstrap the real degrees of freedom toward larger time steps even for these cases, although not likely as large as the 6 fs time step reported here for a simple water model. We will be reporting on these results in the near future.

ACKNOWLEDGMENTS. AA and THG thank the National Science Foundation Grant No. CHE-1363320 and CHE-1665315 for support of this work.

Supporting Information Available: NVE ensemble properties at short time steps, induced dipole probability distributions, induced dipole autocorrelations, and radial distribution functions for all systems for the EL(T,T*), iEL/0-SCF and standard SCF methods.

REFERENCES

1. Wang, L. P.; Chen, J. H.; Van Voorhis, T. Systematic Parametrization of Polarizable Force Fields from Quantum Chemistry Data. *J Chem Theory Comput* **2013,** *9* (1), 452-460.
2. Wang, L. P.; Head-Gordon, T.; Ponder, J. W.; Ren, P.; Chodera, J. D.; Eastman, P. K.; Martinez, T. J.; Pande, V. S. Systematic improvement of a classical molecular model of water. *J Phys Chem B* **2013,** *117* (34), 9956-72.
3. Demerdash, O.; Yap, E. H.; Head-Gordon, T. Advanced potential energy surfaces for condensed phase simulation. *Annu Rev Phys Chem* **2014,** *65*, 149-174.
4. Albaugh, A.; Boateng, H. A.; Bradshaw, R. T.; Demerdash, O. N.; Dziedzic, J.; Mao, Y.; Margul, D. T.; Swails, J.; Zeng, Q.; Case, D. A.; Eastman, P.; Wang, L.-P.; Essex, J. W.; Head-Gordon, M.; Pande, V. S.; Ponder, J. W.; Shao, Y.; Skylaris, C.-K.; Todorov, I. T.; Tuckerman, M. E.; Head-Gordon, T. Advanced Potential Energy Surfaces for Molecular Simulation. *The Journal of Physical Chemistry B* **2016,** *120* (37), 9811-9832.
5. Sprik, M.; Klein, M. L. A Polarizable Model for Water Using Distributed Charge Sites. *Journal of Chemical Physics* **1988,** *89*, 7556-7560.
6. Jacucci, G.; Mcdonald, I. R.; Singer, K. Introduction of Shell-Model of Ionic Polarizability into Molecular-Dynamics Calculations. *Phys Lett A* **1974,** *A 50* (2), 141-143.

7. Mitchell, P. J.; Fincham, D. Shell-Model Simulations by Adiabatic Dynamics. *J Phys-Condens Mat* **1993,** *5* (8), 1031-1038.
8. Lamoureux, G.; MacKerell, A. D.; Roux, B. A simple polarizable model of water based on classical Drude oscillators. *Journal of Chemical Physics* **2003,** *119* (10), 5185-5197.
9. Lamoureux, G.; Roux, B. Modeling induced polarization with classical Drude oscillators: Theory and molecular dynamics simulation algorithm. *Journal of Chemical Physics* **2003,** *119* (6), 3025-3039.
10. Geerke, D. P.; van Gunsteren, W. F. Calculation of the free energy of polarization: Quantifying the effect of explicitly treating electronic polarization on the transferability of force-field parameters. *Journal of Physical Chemistry B* **2007,** *11*, 6425-6436.
11. Yu, H. B.; Hansson, T.; van Gunsteren, W. F. Development of a simple, self-consistent polarizable model for liquid water. *Journal of Chemical Physics* **2003,** *118* (1), 221-234.
12. Rick, S.; Stuart, S.; Berne, B. Dynamical fluctuating charge force-fields: Application to liquid water. *Journal of Chemical Physics* **1994,** *101* (7), 6141-6156.
13. Rick, S. W.; Stuart, S. J.; Bader, J. S.; Berne, B. J. Fluctuating Charge Force-Fields for Aqueous-Solutions. *J Mol Liq* **1995,** *65-6*, 31-40.
14. Patel, S.; Brooks, C. L. CHARMM fluctuating charge force field for proteins: I parameterization and application to bulk organic liquid simulations. *J Comput Chem* **2004,** *25* (1), 1-15.
15. Patel, S.; Mackerell, A. D.; Brooks, C. L. CHARMM fluctuating charge force field for proteins: II - Protein/solvent properties from molecular dynamics simulations using a nonadditive electrostatic model. *J Comput Chem* **2004,** *25* (12), 1504-1514.
16. Kaminski, G. A.; Stern, H. A.; Berne, B. J.; Friesner, R. A.; Cao, Y. X. X.; Murphy, R. B.; Zhou, R. H.; Halgren, T. A. Development of a polarizable force field for proteins via ab initio quantum chemistry: First generation model and gas phase tests. *J Comput Chem* **2002,** *23* (16), 1515-1531.
17. Stern, H. A.; Kaminski, G. A.; Banks, J. L.; Zhou, R. H.; Berne, B. J.; Friesner, R. A. Fluctuating charge, polarizable dipole, and combined models: Parameterization from ab initio quantum chemistry. *Journal of Physical Chemistry B* **1999,** *103* (22), 4730-4737.
18. Warshel, A.; Levitt, M. Theoretical studies of enzymatic reaction: Dielectric, electrostatic, and steric stabilization of carbonium-ion in reaction of lysozyme. *Journal of Molecular Biology* **1976,** *103*, 227-249.
19. Applequist, J.; Carl, J. R.; Fung, K. K. Atom Dipole Interaction Model for Molecular Polarizability - Application to Polyatomic-Molecules and Determination of Atom Polarizabilities. *J Am Chem Soc* **1972,** *94* (9), 2952-&.
20. Thole, B. T. Molecular Polarizabilities Calculated with a Modified Dipole Interaction. *Chem Phys* **1981,** *59* (3), 341-350.
21. Ponder, J. W.; Wu, C.; Ren, P.; Pande, V. S.; Chodera, J. D.; Schnieders, M. J.; Haque, I.; Mobley, D. L.; Lambrecht, D. S.; DiStasio, R. A., Jr.; Head-Gordon, M.; Clark, G. N.; Johnson, M. E.; Head-Gordon, T. Current status of the AMOEBA polarizable force field. *J Phys Chem B* **2010,** *114* (8), 2549-64.
22. Piquemal, J.-P.; Gresh, N.; Giessner-Prettre, C. Improved Formulas for the Calculation of the Electrostatic Contribution to the Intermolecular Interaction Energy from Multipolar Expansion of the Electronic Distribution. *Journal of Physical Chemistry A* **2003,** *107*, 10353-10359.
23. Engkvist, O.; Astrand, P. O.; Karlstrom, G. Accurate intermolecular potentials obtained from molecular wave functions: Bridging the gap between quantum chemistry and molecular simulations. *Chem Rev* **2000,** *100* (11), 4087-4108.

24. Palmo, K.; Mannfors, B.; Mirkin, N. G.; Krimm, S. Inclusion of charge and polarizability fluxes provides needed physical accuracy in molecular mechanics force fields. *Chem Phys Lett* **2006,** *429* (4-6), 628-632.
25. Shao, Y.; Molnar, L.; Jung, Y.; Kussmann, J.; Ochsenfeld, C.; Brown, S.; Gilbert, A.; Slipchenko, L.; Levchenko, S.; O'Neill, D.; DiStasio, R.; Lochan, R.; Wang, T.; Beran, G.; Besley, N.; Herbert, J.; Lin, C.; Van Voorhis, T.; Chien, S.; Sodt, A.; Steele, R.; Rassolov, V.; Maslen, P.; Korambath, P.; Adamson, R.; Austin, B.; Baker, J.; Byrd, E.; Dachsel, H.; Doerksen, R.; Dreuw, A.; Dunietz, B.; Dutoi, A.; Furlani, T.; Gwaltney, S.; Heyden, A.; Hirata, S.; Hsu, C.; Kedziora, G.; Khalliulin, R.; Klunzinger, P.; Lee, A.; Lee, M.; Liang, W.; Lotan, I.; Nair, N.; Peters, B.; Proynov, E.; Pieniazek, P.; Rhee, Y.; Ritchie, J.; Rosta, E.; Sherrill, C.; Simmonett, A.; Subotnik, J.; Woodcock, H.; Zhang, W.; Bell, A.; Chakraborty, A.; Chipman, D.; Keil, F.; Warshel, A.; Hehre, W.; Schaefer, H.; Kong, J.; Krylov, A.; Gill, P.; Head-Gordon, M. Advances in methods and algorithms in a modern quantum chemistry program package. *PHYSICAL CHEMISTRY CHEMICAL PHYSICS* **2006,** *8* (27), 3172-3191.
26. Xie, W. S.; Pu, J. Z.; MacKerell, A. D.; Gao, J. L. Development of a polarizable intermolecular potential function (PIPF) for liquid amides and alkanes. *J Chem Theory Comput* **2007,** *3* (6), 1878-1889.
27. Jorgensen, W. L.; Jensen, K. P.; Alexandrova, A. N. Polarization effects for hydrogen-bonded complexes of substituted phenols with water and chloride ion. *J Chem Theory Comput* **2007,** *3* (6), 1987-1992.
28. Young, D. *Iterative Solutions of Large Linear Systems.* Academic Press: New York, 1971.
29. Wang, W.; Skeel, R. D. Fast evaluation of polarizable forces. *Journal of Chemical Physics* **2005,** *123*, 164107.
30. Aviat, F.; Levitt, A.; Stamm, B.; Maday, Y.; Ren, P.; Ponder, J. W.; Lagardère, L.; Piquemal, J.-P. Truncated Conjugate Gradient: An Optimal Strategy for the Analytical Evaluation of the Many-Body Polarization Energy and Forces in Molecular Simulations. *J Chem Theory Comput* **2017,** *13* (1), 180-190.
31. Simmonett, A. C.; IV, F. C. P.; Ponder, J. W.; Brooks, B. R. An empirical extrapolation scheme for efficient treatment of induced dipoles. *The Journal of Chemical Physics* **2016,** *145* (16), 164101.
32. Simmonett, A. C.; Pickard, F. C.; Shao, Y.; Cheatham, T. E., III; Brooks, B. R. Efficient treatment of induced dipoles. *Journal of Chemical Physics* **2015,** *143* (7).
33. Simmonett, A. C.; Pickard, F. C. t.; Schaefer, H. F., 3rd; Brooks, B. R. An efficient algorithm for multipole energies and derivatives based on spherical harmonics and extensions to particle mesh Ewald. *J Chem Phys* **2014,** *140* (18), 184101.
34. Van Belle, D.; Couplet, I.; Prevost, M.; Wodak, S. J. Calculations of electrostatic properties in proteins. *Journal of Molecular Biology* **1987,** *198* (4), 721-735.
35. Lopes, P. E.; Roux, B.; Mackerell, A. D., Jr. Molecular modeling and dynamics studies with explicit inclusion of electronic polarizability. Theory and applications. *Theor Chem Acc* **2009,** *124* (1-2), 11-28.
36. Albaugh, A.; Demerdash, O.; Head-Gordon, T. An efficient and stable hybrid extended Lagrangian/self-consistent field scheme for solving classical mutual induction. *J Chem Phys* **2015,** *143* (17), 174104.
37. Niklasson, A. M. Extended Born-Oppenheimer molecular dynamics. *Phys Rev Lett* **2008,** *100* (12), 123004.
38. Niklasson, A. M.; Cawkwell, M. J. Generalized extended Lagrangian Born-Oppenheimer molecular dynamics. *J Chem Phys* **2014,** *141* (16), 164123.

39. Niklasson, A. M.; Steneteg, P.; Odell, A.; Bock, N.; Challacombe, M.; Tymczak, C.; Holmström, E.; Zheng, G.; Weber, V. Extended Lagrangian Born–Oppenheimer molecular dynamics with dissipation. *The Journal of chemical physics* **2009,** *130* (21), 214109.
40. Niklasson, A. M.; Tymczak, C. J.; Challacombe, M. Time-reversible Born-Oppenheimer molecular dynamics. *Phys Rev Lett* **2006,** *97* (12), 123001.
41. Niklasson, A. M.; Tymczak, C. J.; Challacombe, M. Time-reversible ab initio molecular dynamics. *J Chem Phys* **2007,** *126* (14), 144103.
42. Albaugh, A.; Niklasson, A. M. N.; Head-Gordon, T. Accurate Classical Polarization Solution with No Self-Consistent Field Iterations. *J Phys Chem Lett* **2017,** *8* (8), 1714-1723.
43. Kolafa, J. Time-reversible always stable predictor–corrector method for molecular dynamics of polarizable molecules. *J Comput Chem* **2004,** *25* (3), 335-342.
44. Ponder, J. W. *Tinker--Software Tools for Molecular Design*, 7.0; 2014.
45. Sprik, M. Computer simulation of the dynamics of induced polarization fluctuations in water. *The Journal of Physical Chemistry* **1991,** *95* (6), 2283-2291.
46. Swope, W. C.; Andersen, H. C.; Berens, P. H.; Wilson, K. R. A computer simulation method for the calculation of equilibrium constants for the formation of physical clusters of molecules: Application to small water clusters. *The Journal of Chemical Physics* **1982,** *76*, 637.
47. Darden, T.; York, D.; Pedersen, L. Particle mesh Ewald : An Nlog(N) method for Ewald sums in large systems. *J. Chem. Phys.* **1993,** *98*, 10089-10092.
48. Andersen, H. C. Rattle: A "velocity" version of the shake algorithm for molecular dynamics calculations. *Journal of Computational Physics* **1983,** *52* (1), 24-34.
49. Martyna, G. J.; Klein, M. L.; Tuckerman, M. Nose-Hoover Chains: the Canonical Ensemble via Continuous Dynamics. *Journal of Chemical Physics* **1992,** *97*, 2635-2643.
50. Ren, P. Y.; Ponder, J. W. Polarizable atomic multipole water model for molecular mechanics simulation. *Journal of Physical Chemistry B* **2003,** *107* (24), 5933-5947.
51. Toukmaji, A.; Sagui, C.; Board, J.; Darden, T. Efficient particle-mesh Ewald based approach to fixed and induced dipolar interactions. *The Journal of Chemical Physics* **2000,** *113* (24), 10913-10927.

TOC Graphic